Characterization of the Mn Oxidation States in Photosystem II by Kβ X-ray Fluorescence Spectroscopy

U. Bergmann,[†] M. M. Grush,[◆] C. R. Horne,[†] P. DeMarois,[§] J. E. Penner-Hahn,[||] C. F. Yocum,[||] D. W. Wright,[⊥] C.E. Dubé,[⊥] W. H. Armstrong,[⊥] G. Christou,[▽] H. J. Eppley,[▽] and S. P. Cramer*[,†,‡]

Lawrence Berkeley National Laboratory, Berkeley, California 94720, Department of Applied Science, University of California, Davis, California 95616, Biophysics Research Division, University of Michigan, Ann Arbor, Michigan 48109, Department of Chemistry, University of Michigan, Ann Arbor, Michigan 48109, Department of Chemistry, Eugene F. Merkert Chemistry Center, Boston College, Chestnut Hill, Massachusetts 02167-3860, and Department of Chemistry, Indiana University, Bloomington, Indiana 47405

Received: April 28, 1998; In Final Form: July 10, 1998

The nature of the Mn oxidation states involved in photosynthetic oxygen evolution has remained controversial, despite intense study by X-ray absorption and electron paramagnetic resonance spectroscopy. As an alternative approach, high-resolution Kβ X-ray fluorescence spectra have been recorded on the dark-adapted S_1 state and the hydroquinone-reduced state of the oxygen-evolving complex in photosystem II. By comparison of the Kβ chemical shifts with those of appropriate model compounds, the S_1 state of photosystem II is found to contain equal amounts of Mn(III) and Mn(IV). In the hydroquinone-reduced sample, a significant fraction of the Mn is reduced to Mn(II). The results are compatible with models involving conversion of $Mn(III)_2Mn(IV)_2$ to $Mn(II)_2Mn(IV)_2$ clusters.

Introduction

The photosynthetic oxidation of water to dioxygen accounts for most of the oxygen in the air we breathe.[1−3] In algae, cyanobacteria, and all higher plants, this reaction is catalyzed by a Mn containing cluster called the oxygen evolving complex (OEC) which is located in photosystem II (PSII).[4,5] The OEC contains four Mn ions, and the catalytic mechanism is proposed to involve five intermediate states called the S states of the Kok cycle.[6] In each of four oxidative steps (S_0-S_4) a photon is absorbed and the OEC is assumed to be singly oxidized; after the last step O_2 is rapidly released and the OEC reverts to S_0. To understand the mechanism of water oxidation, it is critical to know the Mn oxidation states associated with each S-state in this process.

Despite years of study, primarily by EPR[7] and K-edge X-ray absorption spectroscopy,[4] the Mn oxidation states are still a subject of discussion. The S_2 state "multiline" EPR signal, a complex signal centered at $g = 2$ with rich ^{55}Mn hyperfine structure, is often interpreted as an $S = 1/2$ species arising from antiferromagnetic coupling of Mn(III) and Mn(IV) ions. Many have assigned this signal to a $Mn(III)Mn(IV)_3$ cluster, which by inference would make S_1 an even spin species containing $Mn(III)_2Mn(IV)_2$ or $Mn(II)Mn(III)_2Mn(IV)$.[5] In contrast, Zheng and Dismukes have argued for a $Mn(III)_3Mn(IV)$ oxidation state for the S_2 state,[8] and hence a $Mn(III)_4$ assignment for S_1. Most of the K-edge X-ray absorption data for the S_1 state have been interpreted as favoring the $Mn(III)_2Mn(IV)_2$ oxidation state,[9,10] but the X-ray data have also been interpreted as evidence for $Mn(III)_4$.[12]

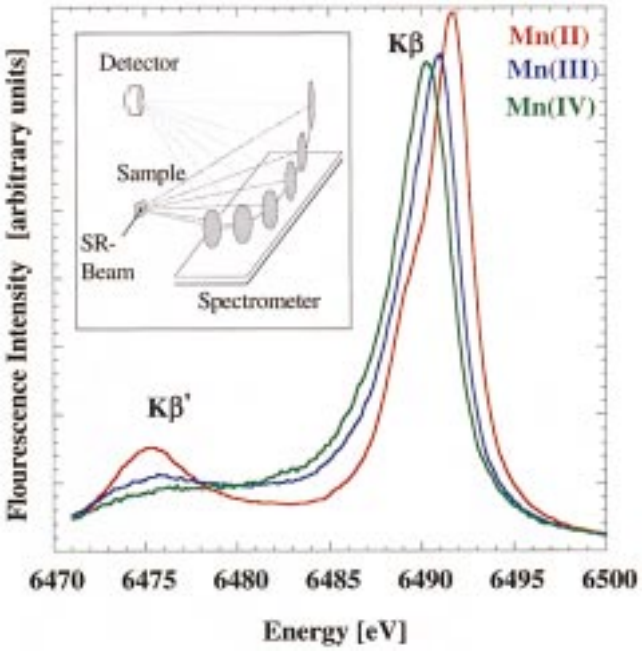

Figure 1. Kβ emission spectra of Mn(II) in MnF_2, Mn(III) in Mn_2O_3, and Mn(IV) in $Mn_4O_6(bpea)_4$. The spectra are normalized to equal integrated intensities. The same normalization was used to determine the ratio of different models to fit the PSII data. The inset shows the schematic experimental setup.

X-ray absorption and EPR both have limitations as techniques for assignment of metal oxidation states. Absorption edge positions are sensitive not only to the charge on the absorbing atom but to the distances and types of neighboring atoms.[13−15] Deriving oxidation state distributions from EPR spectroscopy requires assumptions about reasonable hyperfine tensor elements

* Corresponding author.
[†] Lawrence Berkeley National Laboratory.
[‡] Department of Applied Science.
[§] Biophysics Research Division.
[||] Department of Chemistry, University of Michigan.
[⊥] Department of Chemistry, Eugene F. Merkert Chemistry Center.
[▽] Department of Chemistry, Indiana University.
[◆] Present address: Department of Physics and Astronomy, University of Tennessee, TN 37996.

S1089-5647(98)02038-0 CCC: $15.00
Published on Web 10/15/1998

TABLE 1: Kβ Energies (E_0) and Line Widths (fwhm) of Several Mn Complexes

	name	E_0 [eV]	fwhm [eV]	oxidation state	average	exptl result
1	MnF_2	6491.7	3.78	(II)		
2	Mn_2O_3	6490.9	3.87	(III)		
3	$[Mn_4O_6(bpea)_4](ClO_4)_4$	6490.3	4.03	(IV)		
4	MnO_2	6490.35	4.13	(IV)		
5	Li_2MnO_3	6490.35	4.11	(IV)		
6	$LiMn_2O_4$	6490.5	4.16	(III)(IV)	3.5	3.57
7	$LiMn_{1.9}Ni_{0.1}O_4$	6490.45	4.22	42.1%(III) 57.9%(IV)	3.58	3.71
8	$LiMn_{1.75}Ni_{0.25}O_4$	6490.5	4.23	28.6%(III) 71.4%(IV)	3.71	3.68
9	$Mn_{12}O_{12}(O_2CMe)_{16}(H_2O)_4$	6490.8	4.27	$(III)_8(IV)_4$	3.33	3.25
10	$Mn_{12}O_{12}(O_2CEt)_{16}(H_{2O})_3$	6490.85	4.3	$(III)_8(IV)_4$	3.33	3.20
11	$Mn_{12}O_{12}(O_2CPh)_{16}(H2O)4$	6490.8	4.22	$(III)_8(IV)_4$	3.33	3.28
12	$(PPh)_4[Mn_{12}O_{12}(O_2CEt)_{16}(H_2O)_4]$	6490.87	4.23	$(II)(III)_7(IV)_4$	3.25	3.22
	PSII-S1 control	6490.5	4.29	$(III)_2(IV)_2$ proposed	3.5	3.46
	PSII-S1 H_2Q reduced	6490.7	4.4	$(II)_2(IV)_2$ proposed	3.0	3.0

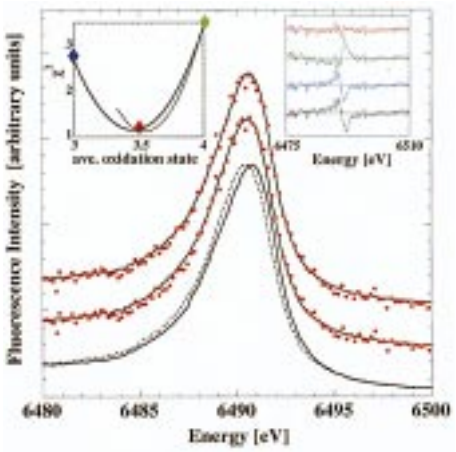

Figure 2. (Top to bottom) Kβ emission spectrum of PSII in the dark-adapted S_1 state and best fit using 50% Mn(III) (Mn_2O_3) and 50% Mn(IV) ($Mn_4O_6(bpea)_4$). Kβ emission spectrum of PSII in the dark-adapted S_1 state compared with $LiMn_2O_4$. Spectrum of $Mn_{12}O_{12}(O_2CEt)_{16}(H_2O)_3$ (solid line) compared with $LiMn_{1.75}Ni_{0.25}O_4$ (dotted line). (Left insert) Values of χ^2 as a function of average oxidation state for two model combinations: models 2 and 3 (solid line) and models 3 and 10 (dotted line). Colored diamonds indicate the average oxidation state and χ^2-value corresponding to the top three difference spectra in the right insert. (Right inset) Difference spectra (fit minus data) using models 1−3, top to bottom: 50% Mn(III) 50% Mn(IV), 100% Mn(III), 100% Mn(IV), 25% Mn(II) 50% Mn(III) 25% Mn(IV).

for the spin Hamiltonians.[8] Clearly it would be valuable to probe the oxidation states of the Mn by a more direct method. We report here the use of high-resolution X-ray fluorescence spectroscopy.

Chemical shifts in Mn Kβ emission spectra (Figure 1) result from a large 3p3d exchange coupling in the final state.[16,17] For high-spin Mn(II), the ^{7}P final state with parallel 3p and 3d spins has a lower energy than the ^{5}P final state, hence the Kβ fluorescence from the ^{7}P state moves to higher energy from the Kβ′-satellite peak. As a consequence of having fewer 3d electrons, the exchange interaction is weaker in Mn(III) and Mn(IV), thus giving Kβ − Kβ′ splittings that are correspondingly smaller. Representative data for a variety of relevant Mn complexes are summarized in Table 1.[18] Although these effects have been recognized for many years,[19,20] it is only with the high flux of modern synchrotron radiation sources that Kβ spectroscopy of dilute metalloproteins has become possible.

Results and Discussion

We recorded the Kβ spectra for Mn in photosystem II (Figure 2) using an array of Si crystal spectrometers (inset Figure 1) and synchrotron radiation excitation.[21] The dark-adapted S_1 sample[22] has a Kβ peak energy E_0 between those of the Mn(III) and Mn(IV) models (see Table 1). The fwhm value is broader than fwhm values of homovalent models and comparable to those of the heterovalent models, suggesting a mixture of oxidation states. To quantitate this apparent mixture, we first fit the PSII spectrum with sums of Mn(III) and Mn(IV) model spectra, allowing their relative intensity to vary as a free parameter. This approach was tested by fitting the heterovalent models 6−12 with mixtures of models 1−3. The results shown in the last column of Table 1 demonstrate that this method consistently reproduces the average oxidation state with an error of less than 0.2.

As shown in the left insert of Figure 2, the best fits for the spectrum of the dark-adapted S_1 sample were obtained with nearly equal amounts of Mn(III) and Mn(IV), and these results did not depend significantly on which Mn(III), Mn(IV), or Mn(III)Mn(IV) containing models were chosen. The top spectrum in Figure 2 shows the fit result of using 50% Mn(III) (Mn_2O_3) and 50% Mn(IV) $[Mn_4O_6(bpea)_4](ClO_4)_4$, and the top three spectra in the right insert show the difference spectra (fit minus data) for the three combinations indicated by the colored diamonds. As can be clearly seen, both the blue (100% Mn(III)) and the green (100% Mn(IV)) spectra show opposite derivative structures, typical for an offset in energy, and only the red spectrum (50% Mn(III) 50% Mn(IV)) indicates good agreement. To furthermore exclude the possibility of a Mn(II)$Mn(III)_2$Mn(IV) cluster, we show the difference spectrum (black) using 25% Mn(II), 50% Mn(III) and 25% Mn(IV) at the bottom of the right insert.

The second spectrum in Figure 2 shows that, in addition to the simulation by mixtures of homovalent compounds, the PSII S_1 spectrum is well simulated ($\chi^2 = 1.27$) by the spectrum of the mixed-valent $LiMn_2O_4$, which contains equal amounts of Mn(III) and Mn(IV).[23] Finally, the two spectra at the bottom of Figure 2 indicate that the Kβ spectra are sufficiently sensitive to distinguish between 3:1 and 1:3 Mn(III):Mn(IV) mixtures. Summarizing our results, the observed Kβ spectrum clearly rules out a homogeneous Mn oxidation state. Assuming that the OEC is a 4 Mn cluster, we conclude that the S_1 state is best described as the $Mn(III)_2Mn(IV)_2$ oxidation state.

Treatment of the OEC with hydroquinone reduces the Mn in a photochemically reversible manner.[24] On the basis of EXAFS and K-edge XANES measurements, this state was suggested to have the unusual $Mn(II)_2Mn(IV)_2$ oxidation state.[24] Kβ emission data support this assignment. The Kβ spectrum becomes broader and shifts to higher energy in the hydroquinone-treated PSII (Figure 3). Given that hydroquinone is expected to behave as a two electron reductant and that Mn(II) is produced by hydroquinone treatment,[24] the proposed $Mn(III)_2Mn(IV)_2$ description of the S_1 state implies $Mn(II)_2Mn(IV)_2$, Mn(II)Mn-

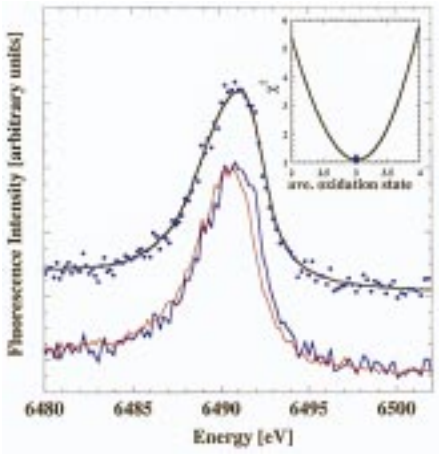

Figure 3. (Top to bottom) Kβ emission spectrum of PSII in the hydroquinone-reduced state and the best fit using 50% Mn(II) (MnF_2) and 50% Mn(IV) ($(Mn_4O_6(bpea)_4)$). Comparison of PSII in the dark-adapted S_1 state (red) and hydroquinone-reduced state (blue). (Inset) values of χ^2 for PSII in the hydroquinone-reduced state as a function of average oxidation state for the combination of models 1 and 3 showing the minimum at 50% Mn(II) and 50% Mn(IV) (blue diamond).

$(III)_2Mn(IV)$ or $Mn(II)_2Mn(III)_2$ oxidation states for the hydroquinone treated sample, with the latter expected only if two sequential hydroquinone reductions take place. The Kβ energy E_0 (Table 1) is consistent with an average Mn(III) oxidation state and approximately 0.5 eV lower than would be expected for $Mn(II)_2Mn(III)_2$ oxidation state. The fwhm of the emission spectrum for the hydroquinone treated sample (Table 1) is inconsistent with a homovalent $Mn(III)_4$ species and argues for the presence of Mn(II), as expected based on EPR measurements.[23] We find a slightly better fit for $Mn(II)_2Mn(IV)_2$ ($\chi^2 = 1.09$) than for $Mn(II)Mn(III)_2Mn(IV)$ ($\chi^2 = 1.14$). This result is in agreement with the observation that approximately half of the Mn becomes EPR detectable as Mn(II) following hydroquinone treatment. The $Mn(II)_2Mn(IV)_2$ oxidation state assignment is best explained with reduction of a Mn(III) dimer to Mn(II), either as an isolated dimer (e.g., within a dimer-of-dimers model) or as part of a tetranuclear cluster. This is consistent with the loss of the 2.7 Å Mn−Mn distance following hydroquinone treatment.[10]

Reduction of Mn(III) rather than Mn(IV) sites, while unusual, has been seen in Mn model chemistry.[25,26] This could reflect intrinsic differences in the reduction potentials, with for example an oxo stabilized Mn(IV) site having a lower reduction potential than a hydroxo-ligated Mn(III). Alternatively, reduction of Mn(III) could occur as a consequence of disproportionation, in which the initial reduction gives a $Mn(III)_4$ state which disproportionates to $Mn(II)_2Mn(IV)_2$. Finally, the observed reduction chemistry could simply reflect limited access of the large hydrophobic hydroquinone to the Mn active site such that only the Mn(III) site can be reduced by hydroquinone.[10]

In conclusion, we find strong evidence for a mixed valence $Mn(III)_2$ $Mn(IV)_2$ cluster in the dark-adapted S_1 state of the OEC. This result is consistent with one of the proposed models for the Mn oxidation states in PSII[3]. One implication is that the S_4 state, which is 3 equivalents more oxidized than S_1, must either involve Mn(V) or an organic radical. For the hydroquinone reduced state our data slightly favor a $Mn(II)_2Mn(IV)_2$ assignment over $Mn(II)Mn(III)_2Mn(IV)$.

Future work will include the study of a wider variety of Mn complexes to address the dependence of the Kβ chemical shifts on parameters such as coordination number and degree of covalency. It is not expected that the Kβ shifts are fully independent of these parameters and the right choice of models will remain an important issue. Nevertheless, it has been demonstrated that Kβ X-ray fluorescence spectroscopy is a valuable tool that complements XAS, and should therefore find many applications in the future.

Acknowledgment. The authors acknowledge the excellent support of Dr. H. Tompkins and his group as well as the Biotech group at SSRL, and Drs. L. E. Berman and Zhijian Yin at NSLS. We thank Dr. A. Rougier for providing the Mn_2O_3 sample. This research was supported by the National Institutes of Health (Grants GM-48145 to SPC, GM-45205 to J.P.H, Grants GM38275 to W.H.A.), Photosynthesis Program of the Competitive Research Grants Office, USDA (Grant G-96-35306-3399 to C.F.Y), and by the Department of Energy, Office of Biological and Environmental Research. The Stanford Synchrotron Radiation Laboratory and the National Synchrotron Light Source are supported by the Department of Energy, Office of Basic Energy Sciences.

References and Notes

(1) Nugent, J. H. A. *Eur. J. Biochem.* **1996**, *237*, 519.
(2) Griffin, K. L.; Seemann, J. R. *Chem. Biol.* **1996**, *3*, 245.
(3) Levanon, H.; Möbius, K. *Annu. Rev. of Biophys. and Biomol. Struct.* **1997**, *26*, 495.
(4) Yachandra, V. K.; Sauer, K.; Klein, M. P. *Chem. Rev.* **1996**, *96*, 2927.
(5) Debus, R. J. *Biochim. Biophys. Acta* **1992**, *1102*, 269.
(6) Kok, B.; Forbush, B.; McGloin, M. *Photochem. Photobiol.* **1970**, *11*, 457.
(7) Brudvig, G. W. In *Advanced EPR: Applications in Biology and Biochemistry*; Hoff, A. J., Ed.; Elsevier: Amsterdam, 1990; pp 839−865.
(8) Zheng, M.; Dismukes, G. C. *Inorg. Chem.* **1996**, *35*, 3307.
(9) Yachandra, V. K.; et al. *Science* **1993**, *260*, 675.
(10) Riggs, P. J.; Mei, R.; Yocum, C. F.; Penner-Hahn, J. E. *J. Am. Chem. Soc.* **1992**, *114*, 10650.
(11) Penner-Hahn, J. E.; et al. *J. Am. Chem. Soc.* **1990**, *112*, 2549.
(12) Kusunoki, M.; Ono, T.; Matsushita, T.; Oyanagi, H.; Inoue, Y. M. N. *J. Biochem.* **1990**, *108*, 560.
(13) Mahto, P.; Chetal, A. R. *Phys. B* **1989**, *158*, 415.
(14) Kasrai, M.; Fleet, M. E.; Bancroft, G. M.; Tan, K. H.; Chen, J. M. *Phys. Rev. B* **1991**, *43*, 1763.
(15) Randall, D. W.; et al. *J. Am. Chem. Soc.* **1995**, *117*, 11780.
(16) Tsutsumi, K. *J. Phys. Soc. Jpn.* **1959**, *14*, 1696.
(17) Peng, G.; et al. *J. Am. Chem. Soc.* **1994**, *116*, 2914.
(18) The values of E_0 are calibrated with respect to the literature value of MnF_2. (See ref 17.)
(19) Sanner, V. H. Ph.D. Thesis, Uppsala University, 1941.
(20) Urch, D. S.; Wood, P. R. *X-ray Spectrom.* **1978**, *7*, 9.
(21) (a) Wang, X.; Grush, M. M.; Froeschner, A. G.; Cramer, S. P. *J. Synchrotron Radiat.* **1997**, *4*, 236. (b) Bergmann, U.; Cramer, S. P. *Proc. SPIE* **1998**. In Press.
(22) Preparation of the PSII-samples was done at the University of Michigan following standard procedures (ref 10.) The samples were kept in darkness in a He flow cryostat at 12 K. The PSII-samples were systematically repositioned during data collection to minimize the effect of photoreduction. A small effect was observed after several hours of exposure and the corresponding spectra were discarded for the data analysis.
(23) Pistoia, G.; Antonini, A.; Rosati, R.; Bellitto, C.; Ingo, G. M. *Chem. Mater.* **1997**, *9*, 1443.
(24) Mei, R.; Yocum, C. F. *Biochemistry* **1992**, *31*, 8449.
(25) Chan, M. K.; Amstrong, W. H. *J. Am. Chem. Soc.* **1990**, *112*, 4985.
(26) Eppley H. J.; et al., *J. Am. Chem. Soc.* **1995**, *117*, 301.